Drug Design, Development and Therapy

Dovepress
Taylor & Francis Group

Open Access Full Text Article

ORIGINAL RESEARCH

Gui-Pi-Tang Defers Skeletal Muscle and Cardiac Muscle Aging by Promoting Mitochondrial Remodeling

Changjiu Cai[1,*], Manying Wang[2,*], Dan Yang[2], Chenxu Jing[2], Yingna Li[3], Hanying Xu[4], Fangbing Liu[5], Daqing Zhao[5]

[1]Jilin Ginseng Academy, Changchun University of Chinese Medicine, Changchun, Jilin, People's Republic of China; [2]Research Center of Traditional Chinese Medicine, Affiliated Hospital to Changchun University of Chinese Medicine, Changchun, Jilin, People's Republic of China; [3]College of Traditional Chinese Medicine, Changchun University of Chinese Medicine, Changchun, Jilin, People's Republic of China; [4]Department of Encephalopathy, Affiliated Hospital of Changchun University of Chinese Medicine, Changchun, Jilin, People's Republic of China; [5]Northeast Asia Institute of Traditional Chinese Medicine, Changchun University of Chinese Medicine, Changchun, Jilin, People's Republic of China

*These authors contributed equally to this work

Correspondence: Fangbing Liu; Daqing Zhao, Northeast Asia Institute of Traditional Chinese Medicine, Changchun University of Chinese Medicine, Changchun, Jilin, People's Republic of China, Email liufb@ccucm.edu.cn; zhaodaqing1963@163.com

Purpose: To determine whether Gui-Pi-Tang (GPT) has protective effects on skeletal muscle and cardiac muscle in aged mice.

Methods: This study used C57BL6/J mice to establish an in vivo natural aging model, while D-galactose (D-gal)-injured C2C12 and H9c2 cells were employed to create in vitro aging cell models. Hematoxylin and eosin (H&E) staining was used to assess the effect of GPT on skeletal and cardiac muscle in aged mice. Protection against age-induced cellular damage by GPT was assessed in C2C12 and H9c2 cells using β-galactosidase staining. Mitochondrial morphology, structure, and function were analyzed using transmission electron microscopy, Seahorse assays, and ATP content measurements. Potential mechanisms by which GPT regulates mitochondrial homeostasis were examined using Western blot analysis.

Results: GPT treatment significantly improved the alignment of skeletal muscle fibers, reduced gaps, and increased the cross-sectional area (CSA) of skeletal muscle in aged mice. It also reduced the CSA of cardiac muscle fibers, alleviating cardiomyocyte hypertrophy. Mitochondrial morphology was restored, and GPT reduced D-gal-induced β-galactosidase elevation. Furthermore, GPT protected mitochondrial morphological and structural integrity in the skeletal and cardiac muscles of aged mice and improved mitochondrial respiratory function and ATP levels in D-gal-injured C2C12 and H9c2 cells. GPT treatment increased the levels of mitochondrion-associated proteins PGC-1α, PPARγ, Nrf1, and OPA1 in the skeletal and cardiac muscle of aged mice. Moreover, GPT modulated Drp1 expression, with increases in aged skeletal muscle and decreases in aged cardiac muscle.

Conclusion: These findings suggest that GPT helps maintain mitochondrial homeostasis by regulating mitochondrial remodeling, thereby alleviating skeletal and cardiac muscle damage in aged mice.

Keywords: Gui-Pi-Tang, mitochondrial homeostasis, skeletal muscle, myocardium, senescence

Introduction

Global demographics have shifted significantly due to medical advancements, leading to an accelerated increase in the elderly population. Projections estimate that the number of people over 60 will increase to twice its current number by 2050.[1] Aging is directly associated with various chronic human diseases, including cancer, diabetes mellitus, cardiovascular diseases (CVDs), cerebrovascular disorders, and neurological diseases.[2] In addition to presenting significant challenges for governments and healthcare systems, aging negatively affects the quality of life for the elderly. Therefore, delaying the aging process has become an urgent need.

Received: 28 November 2024
Accepted: 9 April 2025
Published: 21 April 2025

Graphical Abstract

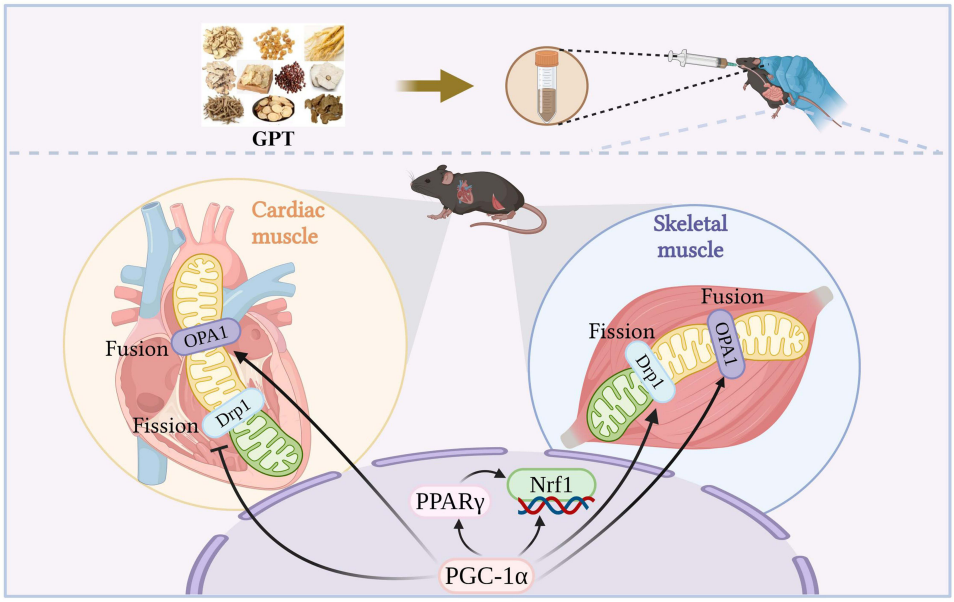

Previous research has identified 12 key characteristics of aging,[3] with mitochondrial dysfunction being one of the most critical factors. Mitochondria are the primary organelles involved in energy generation, and mitochondrial dysfunction significantly impacts various tissues and organs in the body.[4] Skeletal muscle atrophy and cardiac hypertrophy occur during the aging process; both these tissues have the largest numbers and percentages of mitochondria.[5] Therefore, it is reasonable to assume that mitochondrial dysfunction may play a key role in skeletal muscle atrophy and cardiac hypertrophy and even heart failure associated with aging.

Mitochondria are vital organelles characterized by a unique bilayer membrane structure. Mitochondria undergo two dynamic processes: fusion, where two adjacent mitochondria connect, and fission, where one mitochondrion divides into two. These processes balance each other, maintaining mitochondrial homeostasis. When this balance is disrupted, caused by downregulation of one process and consequent upregulation of the other, mitochondrial homeostasis becomes compromised, resulting in functional decline or even loss.[6] Research has demonstrated varying effects of mitochondrial fission and fusion on lifespan. For instance, increased mitochondrial fission has been shown to extend yeast lifespan but reduce that of nematodes.[7] In contrast, studies on *Caenorhabditis elegans* and *Drosophila melanogaster* have found that higher levels of mitochondrial fusion are linked to with extended lifespan.[8] Mitochondrial loss results in insufficient ATP production, leading to reduced protein synthesis and accelerated degradation in skeletal muscles and subsequent atrophy of muscle fibers, while cardiomyocytes in cardiac muscle are forced to undergo compensatory hypertrophy to maintain the pumping function of the heart.[9] While there are differences between single-celled and multicellular organisms, these findings collectively highlight the critical importance of maintaining mitochondrial dynamics to preserve mitochondrial function.

Gui-Pi-Tang (GPT) is a traditional Chinese medicine prescription composed of several key ingredients, including *Astragalus mongholicus* Bunge, and *Dimocarpus longan* Lour, (Jun), *Panax ginseng* C. A. Mey, *Atractylodes macrocephala* Koidz., *Angelica sinensis* (Oliv). Diels, *Ziziphus jujuba* (Chen), *Poria cocos* (Schw). Wolf, *Polygala tenuifolia* Willd, *Glycyrrhiza uralensis* Fisch (Zuo), and *Aucklandia lappa* DC (Shi). It is traditionally used to replenish qi, nourish the blood, and invigorate heart and spleen functions. Previous research has demonstrated GPT's ability to extend the lifespan of fruit flies,[10] protect mitochondria, and alleviate liver damage caused by the alcohol extract of *Tripterygium wilfordii* in rats.[11] Furthermore, GPT has been shown to reduce oxidative stress in skeletal muscle mitochondria and improve chemotherapy-related fatigue.[12] This

evidence suggests that GPT may be able to protect mitochondria and delay aging. To explore this, the components of GPT were evaluated using liquid chromatography-mass spectrometry (LC-MS), and aging models were established using naturally aged mice and D-gal-injured C2C12 and H9c2 cells. This approach aims to elucidate the components and potential mechanisms of GPT in delaying the aging of skeletal and cardiac muscles.

Materials and Methods

Preparation of GPT Extracts

The GPT extract was formulated from ten traditional medicinal herbs (Table 1), procured from the Department of Pharmacy at the Affiliated Hospital of Changchun University of Chinese Medicine (Jilin, China). Following standard protocols outlined in the Chinese Pharmacopoeia 2015 edition, 1.91 L of reverse osmosis water was combined with 30 g of Huangqi (*Astragalus mongholicus* Bunge, Fabaceae, Root), 30 g of Longan (*Dimocarpus longan* Lour, Sapindaceae, Fruit pulp), 15 g of Renshen (*Panax ginseng* C. A. Mey, Araliaceae, Root), 30 g of Baizhu (*Atractylodes macrocephala* Koidz, Asteraceae, Root), 3 g of Danggui (*Angelica sinensis* (Oliv). Diels, Apiaceae, Root), 30 g of Suanzaoren (*Ziziphus jujuba*, Rhamnaceae, Seed), 30 g of Fushen (*Poria cocos* (Schw). Wolf, Polyporaceae, Sclerotium), 3 g of Yuanzhi (*Polygala tenuifolia* Willd, Polygalaceae, Root), 5 g of Gancao (*Glycyrrhiza uralensis* Fisch, Fabaceae, Root), and 15 g of Muxiang (*Aucklandia lappa* DC, Asteraceae, Root). Simmering and reduction at 100°C for 30 min resulted in a volume of 300 mL. Three extractions were performed to ensure maximum yield. The aqueous extracts were filtered and centrifuged (8,000 rpm, 15 min, 4°C), followed by freeze-drying under vaccum. The final extraction yield of the experimental drug was 39.93%.

Ultra-High-Performance Liquid Chromatography (UHPLC) Analysis of GPT

The resulting powder was dissolved in ddH_2O to a concentration of 100 mg/mL, followed by filtration using a 0.2 μm membrane, sterilization, and dilution for further experiments. UHPLC analysis was undertaken to verify the quality of the GPT extract before its use in experiments. GPT sample (100 mg) was mixed with 70% methanol (1 mL) and ground using a JXFSTPRP-48 homogenizer at 70 hz. After shaking for 3 minutes, the mixture was subjected to low-temperature ultrasonication at 40 kHz. After centrifugation (12,000 rpm, 10 min, 4°C), the supernatant was filtered through 0.22 μm PTFE membrane before UHPLC analysis was performed using a Thermo Vanquish UHPLC system (Thermo Fisher, MA, USA) with a Zorbax Eclipse C18 column (1.8 μm x 2.1 mm x 100 mm) (Agilent Technologies, CA, USA) at 30°C, with a mobile phase consisting of 0.1% formic acid in water (A) and acetonitrile (B) at a flow rate of 0.3 mL/min. Tandem mass spectrometry was conducted using a Q-Exactive HF mass spectrometer (ThermoFisher).[13]

Table 1 Composition of the Gui-Pi-Tang Formula

Chinese Name	Latin Name	Family	Part Used	Weight (g)	Voucher Numbers
Huangqi	*Astragalus mongholicus* Bunge	Fabaceae	Root	30	C204240405
Longan	*Dimocarpus longan* Lour.	Sapindaceae	Fruit pulp	30	C269240301
Renshen	*Panax ginseng* C. A. Mey.	Araliaceae	Root	15	C342240401
Baizhu	*Atractylodes macrocephala* Koidz.	Asteraceae	Root	30	C018240102
Danggui	*Angelica sinensis* (Oliv). Diels.	Apiaceae	Root	3	C093240405
Suanzaoren	*Ziziphus jujuba*	Rhamnaceae	Seed	30	231202
Fushen	*Poria cocos* (Schw). Wolf. [Pavhyma cocos Fr.]	Polyporaceae	Sclerotium	30	240401CP217
Yuanzhi	*Polygala tenuifolia* Willd.	Polygalaceae	Root	3	23102301
Gancao	*Glycyrrhiza uralensis* Fisch.	Fabaceae	Root	5	C140240502
Muxiang	*Aucklandia lappa* DC.	Asteraceae	Root	15	C305240401

https://doi.org/10.2147/DDDT.S509046

Mouse Modeling and Treatment

Young (2 months old, n = 6) and aged (18 months old, n = 24) C57BL6/J mice (BIOCYTOGEN, Beijing, China) were kept with unrestricted access to water and standard chow. Mice in the aged group were randomized into four subgroups and administered either PBS or different concentrations of GPT: The clinical dose of GPT used in humans is 191 g/60 kg/d, and this was converted to approximately 39.16 g/kg/d in mice with a proportion of 12.3 times based on the body surface area. This dose was selected for the medium-dose group.[14] The low, medium, and high doses were calculated by two-fold ratios, resulting in 19.58, 39.16 and 78.32 g/kg/d, respectively. The dosage of the freeze-dried powder to GPT-L (7.5 g/kg), GPT-M (15 g/kg), or GPT-H (30 g/kg) was calculated according to the GPT extraction rate of 39.93%. After 4 weeks, all animal procedures were performed following the principles approved by the Animal Ethics Committee of Changchun University of Chinese Medicine (approval no 2022476). On completion of treatment, the mice were euthanized, and sections of the gastrocnemius muscle and heart were harvested for histological, electron microscopy, and Western blot (WB) analyses.

Histological Analyses

The harvested spleen, stomach, intestine, and skeletal and cardiac muscle tissues were fixed in 10% formalin solution in phosphate buffer (pH 7.4, 0.1 M), followed by H&E staining. The sections were evaluated and imaged using a light microscope (BX53, Olympus, Japan).

Cell Culture and Treatment

C2C12 and H9c2 cell lines, purchased from the American Type Culture Collection (VA, USA), were grown in Dulbecco's Modified Eagle Medium (DMEM) supplemented with 10% fetal bovine serum (FBS), 25 mm glucose, and penicillin/streptomycin in a 5% CO_2 incubator.[15] The cells were divided into five experimental groups: (1) the control group, where cells were grown for 48 hours in a complete medium; (2) the model group, where cells were treated with D-galactose (D-gal) for 48 hours; (3–5) treatment groups, where cells were exposed to D-gal and GPT at 50, 100, or 200 μg/mL for 48 hours.

SPiDER-β-Gal Detection

Cellular senescence was assessed using SPiDER-β Gal staining solution (DOJINDO, Japan, SG03). C2C12 and H9c2 cells (5×10^4 cells/mL) were inoculated in 96-well plates and grown overnight in a 5% CO_2 incubator at 37°C. After washing with HBSS, cells were treated with Bafilomycin A1 working solution and incubated for 1 hour in a 5% CO_2 incubator at 37°C. SPiDER-β Gal working solution was then added and the cells were incubated for 30 min as above. After washing with HBSS, the cells were evaluated and imaged under a fluorescence microscope to assess senescence.

Transmission Electron Microscopy (TEM)

Skeletal muscle and cardiac muscle tissues were fixed in glutaraldehyde (2.5%) for 2 hours, post-fixed with osmium tetroxide (OsO_4), dehydrated, and embedded in Epon resin. Sections (ultrathin) were cut using an Ultra 45° microtome (Daitome, Japan) and stained with uranyl acetate and lead citrate. The sections were examined using a Tecnai G2 20 TWIN TEM (FEI, USA). Image-Pro Plus 6.0 (Media Cybernetics, Inc., MD, USA) was used for image analysis, and all analyses were performed by a statistician blinded to experimental groupings.[16]

Seahorse Assays

Mitochondrial oxygen consumption rates were determined using the Seahorse Bioscience XFp Extracellular Flux Analyzer (Agilent).[17] C2C12 and H9c2 cells were grown in Seahorse XF96 plates for 24 hours before being treated with D-gal and/or GPT. Mitochondrial respiration was evaluated following the introduction of oligomycin (1 μM), FCCP (3 μM for C2C12, 5 μM for H9c2), and rotenone/antimycin A (1 μM).

Intracellular ATP Level Measurement

Cells were treated with GPT and/or D-gal for specified time intervals. After treatment, cells were lysed using an ATP lysis buffer containing 0.5% Triton X-100 and 100 mm glycine (pH 7.4). After centrifugation (15,000 ×g, 10 min),[18] the supernatants were collected. Intracellular levels of ATP were measured using an ATP Bioluminescent Assay Kit (Promega, WI, USA).

Western Immunoblotting

Following two rinses with chilled PBS, cells were lysed for 30 minutes on ice with RIPA buffer (Beyotime Biotechnology, Shanghai, China) and protein quantification was performed with a BCA kit (Beyotime Biotechnology). Thirty microgram protein samples were electrophoresed on 12% SDS-PAGE gels and transferred onto membranes. After blocking (5% skim milk), the blots were treated overnight at 4°C with primary antibodies. HRP-conjugated secondary antibodies were applied for 1 hour.[19] Primary antibodies against PGC-1α, PPARγ, OPA1, Drp1, Nrf1, and GAPDH were obtained from Cell Signaling Technology (MA, USA). Protein bands were visualized using chemiluminescence reagents (Santa Cruz Biotechnology, TX, USA).

Statistical Analyses

Statistical comparisons were conducted using one-way ANOVA followed by Tukey's post hoc test in GraphPad Prism 7.0. Results are presented as means ± SD, with statistical significance defined as $P < 0.05$.

Results

UHPLC-MS/MS Analysis of GPT

A UHPLC-coupled Q-Exactive HF system, along with Compound Discoverer 3.3 software, was used to analyze the chemical composition of GPT. The total ion chromatograms and corresponding values related to quasi-molecular ions, masses, fragment ions, and retention times are given in Figure 1A and B and Table 2.

Effects of GPT on Aged Mice

To assess the influence of GPT on aged mice, 18-month-old female C57BL/6J mice were acclimated for one week and then were gavaged with GPT at varying concentrations (7.5, 15, and 30 g/kg). After four weeks of treatment, the mice were euthanized (Figure 2A). Based on the efficacy of GPT in tonifying the spleen and nourishing the heart, we evaluated its effects on the spleen, stomach, intestine, skeletal muscle, and cardiac muscle using HE staining (Figure 2B). Compared with the aged mice, the spleen cells were found to be closely arranged with clear boundaries between the red and white pulp in the GPT treatment groups (Figure 2C). In the stomach, infiltration of neutrophils and mononuclear inflammatory cells was observed in the mucosa and submucosa of the aged mice. Compared with aged group, medium doses of GPT (15 g/kg) resulted in little improvement. Damage to the intestinal mucosal tissues and structures, together with atrophy and sparsely arranged cells, were visible in the tissues of aged mice, with slight improvements seen following GPT treatment. In aged skeletal muscle, gaps between muscle fibers were enlarged, fiber arrangements were loosened, muscle atrophy was observed, and the CSA was significantly reduced. In the GPT treatment groups, the arrangement of skeletal muscle fibers became more orderly, the gaps between fibers decreased, and the CSA was significantly increased (Figure 2D). Aged cardiac muscle cells exhibited hypertrophy, disordered arrangement, and a significant increase in CSA. GPT treatment significantly alleviated cardiac muscle hypertrophy and reduced the CSA (Figure 2E). Skeletal and cardiac muscle tissues were collected from mice and weighed. The results showed that compared to young mice, aged mice exhibited reduced weights of skeletal muscles and increased weights of cardiac muscles. After GPT treatment, the skeletal muscle weight was found to be significantly increased, while the cardiac muscle weight was decreased in the treated mice relative to the untreated aged mice (Figure 2F). Calculation of the organ coefficients showed that these values were reduced in skeletal muscle and increased in cardiac muscle in aged mice compared to young mice. GPT could thus increase the skeletal muscle organ coefficient and decrease the cardiac muscle organ coefficient in aging mice compared to the untreated aged mice (Figure 2G).

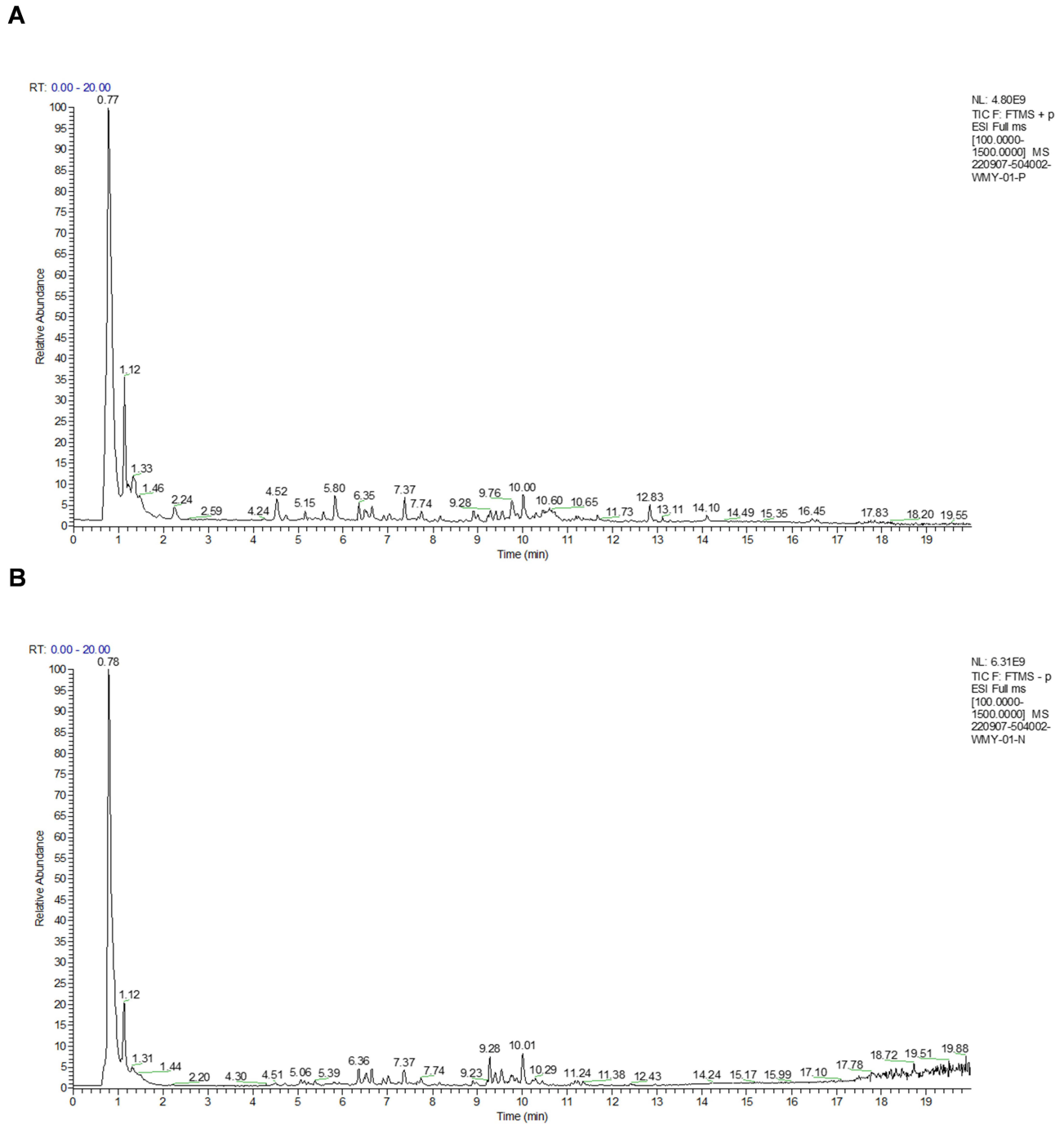

Figure 1 Total ion chromatograms for GPT obtained on a UHPLC-Q-Exactive HF platform in (**A**) positive and (**B**) negative ion modes.

These findings suggest that GPT has protective effects on the spleen, skeletal muscle, and cardiac muscle in aged mice.

Effect of GPT on D-Gal-Injured C2C12 and H9c2 Cells

In vitro experiments were performed to observe the effects of GPT on C2C12 and H9c2 cells. Cells were treated with varying concentration of GPT (25 to 400 μg/mL) for 24–48 hours. MTT assays indicated that GPT was non-toxic to C2C12 and H9c2 cells (Figure S1A and B). To establish an in vitro aging model, C2C12 and H9c2 cells were treated with -gal at various concentrations. MTT results showed that 30 mg/mL D-gal significantly reduced the survival rate of

Table 2 The Chemical Components of GPT

No.	RT (min)	Compounds	Plant Source	Molecular Formula	Expected Neutral Mass (Da)	Observed Neutral Mass (Da)	LC/MS (ESI±) (m/z)	Mass Accuracy (ppm)	Adducts
1	0.77	L-Iditol	Gancao	$C_6H_{14}O_6$	182.07904	182.0787	183.08582	−1.84	$[M+H]^+$
2	0.772	Choline	Danggui[20]	$C_5H_{13}NO$	103.09971	103.09981	104.10706	0.95	$[M+H]^+$
3	0.781	L-Threonine	Huangqi	$C_4H_9NO_3$	119.05824	119.05814	120.06543	−0.87	$[M+H]^+$
4	0.798	Betaine	Huangqi	$C_5H_{11}NO_2$	117.07898	117.07885	118.08614	−1.13	$[M+H]^+$
5	0.808	Trigonelline HCl	Huangqi	$C_7H_7NO_2$	137.04768	137.04733	138.05460	−2.51	$[M+H]^+$
6	0.814	5-Hydroxymethylfurfural	Baizhu	$C_6H_6O_3$	126.03169	126.03149	127.03880	−1.59	$[M+H]^+$
7	1.128	Maltopentaose	Renshen[21]	$C_{30}H_{52}O_{26}$	828.27468	828.2732	827.26611	−1.79	$[M-H]^-$
8	1.175	Uridine	Baizhu[22]	$C_9H_{12}N_2O_6$	244.06954	244.06865	243.06134	−3.61	$[M-H]^-$
9	6.671	Ellagic acid	Longyan[23]	$C_{14}H_6O_8$	302.00627	302.00542	300.99814	−2.81	$[M-H]^-$
10	4.454	Chlorogenic acid	Muxiang[24]	$C_{16}H_{18}O_9$	354.09508	354.09427	355.10123	−2.29	$[M-H]^-$
11	5.234	7-Hydroxycoumarine	Muxiang	$C_9H_6O_3$	162.03169	162.03128	163.03854	−2.58	$[M+H]^+$
12	5.395	Cryptochlorogenic acid	Danggui	$C_{16}H_{18}O_9$	354.09508	354.09419	353.08682	−2.52	$[M-H]^-$
13	5.405	Sibiricose A6	Yuanzhi	$C_{23}H_{32}O_{15}$	548.17412	548.1731	547.16583	−1.86	$[M-H]^-$
14	6.646	Isoliquiritigenin	Gancao[25]	$C_{15}H_{12}O_4$	256.07356	256.07268	257.07996	−3.43	$[M+H]^+$
15	6.662	Liquiritin	Gancao	$C_{21}H_{22}O_9$	418.12638	418.12548	419.13217	−2.15	$[M+H]^+$
16	6.896	7-Methoxycoumarin	Danggui	$C_{10}H_8O_3$	176.04734	176.04692	177.05420	−2.38	$[M+H]^+$
17	6.913	Isochlorogenic acid B	Muxiang	$C_{25}H_{24}O_{12}$	516.12678	516.12552	515.11829	−2.43	$[M-H]^-$
18	7.023	Spinosin B	Suanzaoren[26]	$C_{38}H_{40}O_{18}$	784.22146	784.22021	783.21295	−1.6	$[M-H]^-$
19	7.052	3',6-Disinapoyl sucrose	Yuanzhi[27]	$C_{34}H_{42}O_{19}$	754.23203	754.23025	753.22296	−2.36	$[M-H]^-$
20	7.246	Isochlorogenic acid C	Huangqi	$C_{25}H_{24}O_{12}$	516.12678	516.12541	515.11841	−2.65	$[M+H]^+$
21	7.363	Ginsenoside B2	Renshen	$C_{48}H_{82}O_{18}$	946.55012	946.54799	945.54028	−2.24	$[M-H]^-$
22	7.373	Ginsenoside Rh4	Renshen	$C_{36}H_{60}O_8$	620.42882	620.42714	638.46124	−2.71	$[M+H]^+$
23	7.545	Tenuifoliside A	Yuanzhi	$C_{31}H_{38}O_{17}$	682.2109	682.20986	681.20258	−1.52	$[M-H]^-$
24	7.667	Isoliquiritin	Gancao	$C_{21}H_{22}O_9$	418.12638	418.1249	417.11844	−3.54	$[M+H]^+$
25	8.24	Methylnissolin-3-O-glucoside	Huangqi	$C_{23}H_{26}O_{10}$	462.1526	462.15114	480.18497	−3.16	$[M+H]^+$
26	8.479	Isomucronulatol 7-O-glucoside	Huangqi	$C_{23}H_{28}O_{10}$	464.16825	464.16707	463.15994	−2.53	$[M-H]^-$
27	8.739	Liquiritigenin	Gancao[25]	$C_{15}H_{12}O_4$	256.07356	256.07273	255.06554	−3.24	$[M+H]^+$
28	8.899	Calycosin	Huangqi[28]	$C_{16}H_{12}O_5$	284.06847	284.06747	283.06039	−3.52	$[M+H]^+$
29	9.278	Ginsenoside Rg5	Renshen	$C_{42}H_{70}O_{12}$	766.48673	766.48473	767.49200	−2.6	$[M+H]^+$
30	9.28	Ginsenoside Rk2	Renshen	$C_{36}H_{60}O_7$	604.4339	604.43237	605.43964	−2.54	$[M+H]^+$
31	9.585	20(R)-Ginsenoside Rg2	Renshen	$C_{42}H_{72}O_{13}$	784.49729	784.49623	783.48920	−1.36	$[M-H]^-$
32	10.008	Diammonium glycyrrhizinate	Gancao	$C_{42}H_{62}O_{16}$	822.40379	822.40097	823.40820	−3.43	$[M+H]^+$
33	10.152	Octyl gallate	Longan	$C_{15}H_{22}O_5$	282.14672	282.14589	281.13861	−2.96	$[M-H]^-$
34	10.445	Formononetin	Huangqi	$C_{16}H_{12}O_4$	268.07356	268.07261	269.07986	−3.54	$[M+H]^+$
35	11.058	Medicarpin	Huangqi	$C_{16}H_{14}O_4$	270.08921	270.08836	271.09564	−3.13	$[M+H]^+$
36	11.196	Ginsenoside Rg3	Renshen	$C_{42}H_{72}O_{13}$	784.49729	784.49616	783.48889	−1.44	$[M-H]^-$
37	11.668	Atractylenolide III	Baizhu	$C_{15}H_{20}O_3$	248.14124	248.14048	249.14769	−3.06	$[M+H]^+$
38	12.51	Ligustilide	Danggui	$C_{12}H_{14}O_2$	190.09938	190.09881	191.10608	−3.01	$[M+H]^+$

Abbreviation: RT, retention time.

C2C12 cells after 24–48 hours, with more significant effects after 48 hours (Figure S1C). Similarly, 50 mg/mL D-gal significantly decreased the survival rate of H9c2 cells after 48 hours (Figure S1D). GPT was then used to assess its protective effect on D-gal-injured C2C12 and H9c2 cells. GPT at concentrations of 25–200 μg/mL significantly restored the survival rate of D-gal-injured C2C12 cells after 48 hours, with optimal effects observed at concentrations of 50–200 μg/mL (Figure 3A). In H9c2 cells, GPT at 50–400 μg/mL concentrations significantly improved the survival

https://doi.org/10.2147/DDDT.S509046

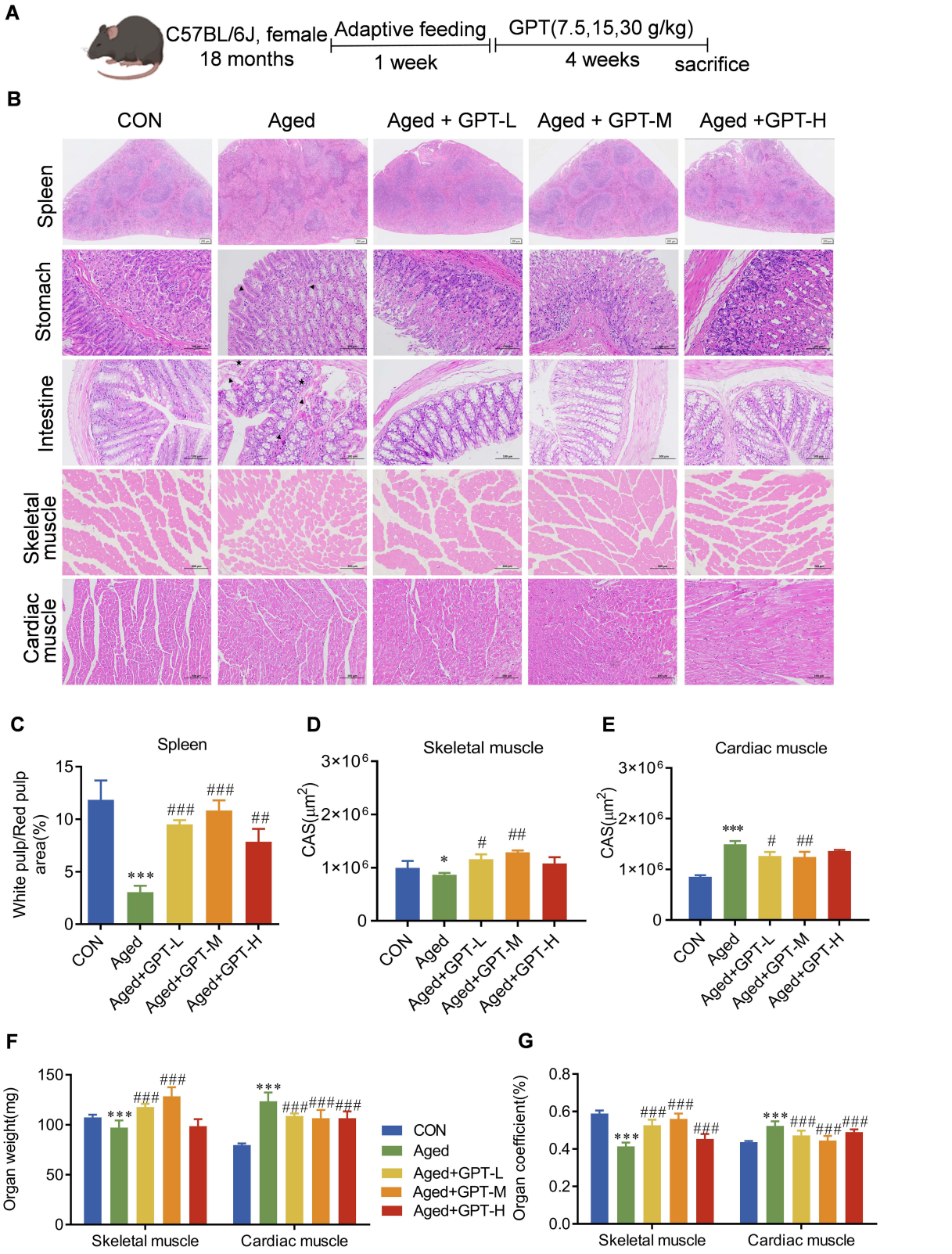

Figure 2 Protective effects of GPT in skeletal and cardiac muscles of aged mice. (**A**) Schedule of animal experiments. (**B**) Morphological changes in spleen (scale bar = 100 μm), stomach (scale bar = 100 μm), intestine (scale bar = 100 μm), skeletal muscle (scale bar = 200 μm) and cardiac muscle (scale bar = 100 μm) were assessed by H&E staining. "▲" indicates infiltration of neutrophils and mononuclear inflammatory cells in the mucosa or submucosa. "★" indicates the degeneration or necrosis of mucosal epithelium. (**C**) White/red pulp area of the spleen. (**D** and **E**) CSA analysis of H&E staining for skeletal and cardiac muscles. (**F**) Organ weights of skeletal and cardiac muscles. (**G**) Organ coefficients of skeletal and cardiac muscles. Data represent means ± SD (n = 5). Compared with the control group: $^{*}P < 0.05$, $^{***}P < 0.001$; compared with the model group: $^{\#}P < 0.05$, $^{\#\#}P < 0.01$, $^{\#\#\#}P < 0.001$.

https://doi.org/10.2147/DDDT.S509046

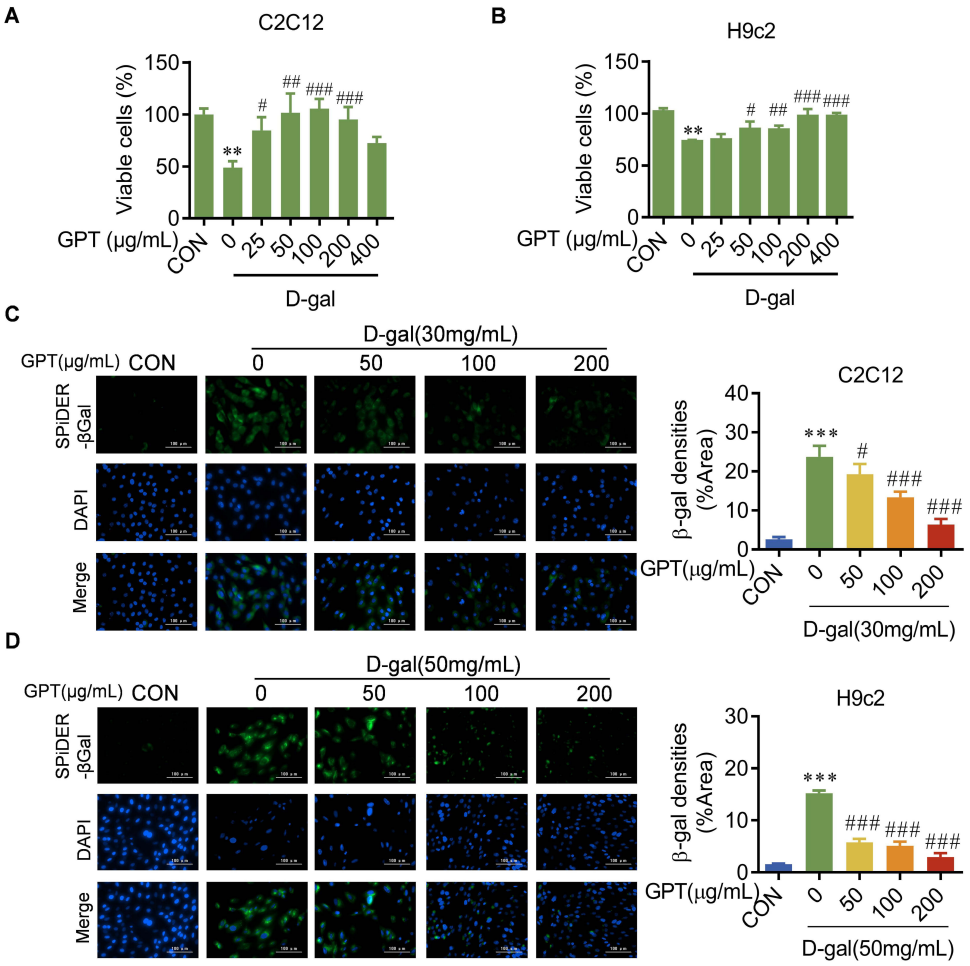

Figure 3 Protective effects of GPT in D-gal-injured C2C12 and H9c2 cells. (**A** and **B**) MTT assays were used for measuring the effect of GPT on the survival of D-gal-injured C2C12 and H9c2 cells. (**C** and **D**) Representative images of SA-β-gal staining in D-gal injured C2C12 and H9c2 cells incubated with GTP for 48 h. Scale bar = 100 μm. Data (n = 5) represent means ± SD. Compared with the control group: $^{**}P < 0.01$, $^{***}P < 0.001$; compared with the model group: $^{\#}P < 0.05$, $^{\#\#}P < 0.01$, $^{\#\#\#}P < 0.001$.

rate of D-gal-injured cells (Figure 3B). β-galactosidase (SA-β-gal) is a senescence marker.[29] Our results demonstrated that GPT reduced SA-β-gal accumulation in both D-gal-injured C2C12 and H9c2 cells (Figure 3C and D). These findings suggest that GPT shows protective effects in D-gal-injured C2C12 and H9c2 cells.

Effect of GPT on Mitochondrial Function in Skeletal Muscle of Aged Mice and D-Gal Injured C2C12 Cells

Mitochondria are important cellular organelles responsible for energy production, and their morphology, structure, and arrangement are essential for maintaining their function.[30] Electron microscopy analysis revealed significant mitochondrial damage in the skeletal muscle of aged mice, including ruptured mitochondrial membranes, dissolved inner cristae, and vacuolation. Treatment with GPT significantly improved these mitochondrial defects in the muscle tissues of aged mice (Figure 4A). Further analysis of mitochondrial function in C2C12 cells using Seahorse assays demonstrated that D-gal treatment impaired both basal and maximal mitochondrial respiration compared to the control group. GPT treatment effectively restored these respiration metrics to near-normal levels (Figure 4B–D). Furthermore, ATP assays indicated that GPT significantly enhanced ATP production in D-gal-injured C2C12 cells (Figure 4E). Electron microscopy of D-gal-injured C2C12 cells further confirmed the protective effects of GPT, as mitochondrial damage was visibly reduced following GPT treatment (Figure 4F). These findings indicate that GPT has protective effects on mitochondrial function, both in vivo in skeletal muscle of aged mice and in vitro in D-gal-injured C2C12 cells, effectively restoring mitochondrial integrity and functionality.

https://doi.org/10.2147/DDDT.S509046

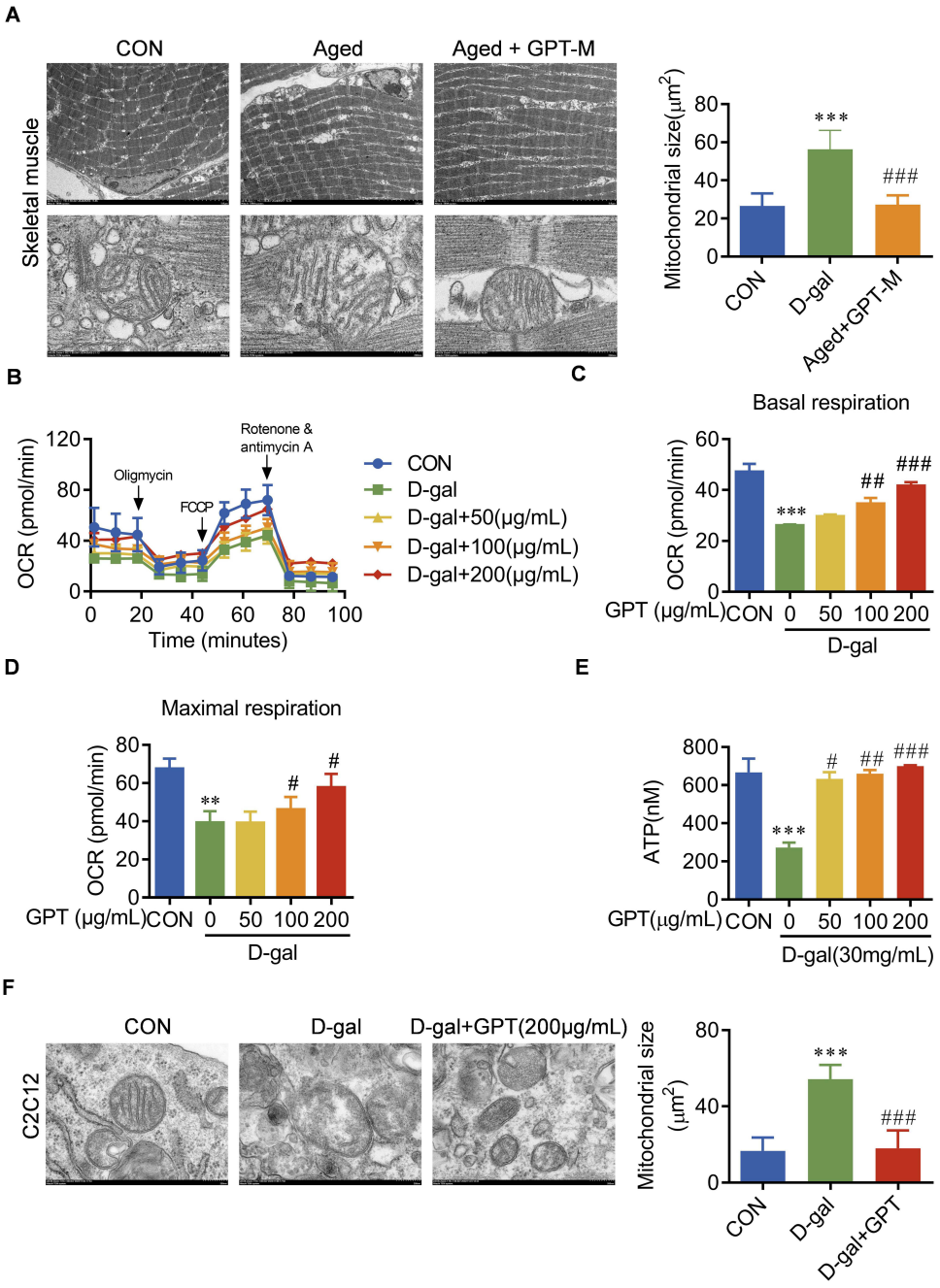

Figure 4 Effect of GPT on mitochondrial function in skeletal muscles of aged mice and D-gal injured C2C12 cells. (**A**) Ultrastructure (2,500×) and electron microscopy images (40,000×) of mitochondria in skeletal muscle. Mitochondrial area statistics (n = 5). (**B**) Seahorse curves of mitochondrial stress experiments in C2C12 cells. (**C** and **D**) Basal respiration and Maximal respiration of Seahorse curves. (**E**) ATP production in C2C12 cells. (**F**) Mitochondrial images (40,000×) and mitochondrial area statistics (n = 3) of C2C12 cells. Compared with control group, $^{**}P < 0.01$, $^{***}P < 0.001$; compared with the model group: $^{\#}P < 0.05$, $^{\#\#}P < 0.01$, $^{\#\#\#}P < 0.001$.

GPT Protects Mitochondrial Function in Cardiac Muscle of Aged Mice, and D-Gal Injured H9c2 Cells

Mitochondria are abundant in cardiac muscle, and mitochondrial dysfunction has been implicated in both heart failure and the aging process. It is also a major contributor to cardiac aging.[31] Our experiments showed that cardiac mitochondria showed normal structure in young mice, with well-organized cristae and electron-dense matrix. In contrast, aged mice demonstrated enlarged and swollen mitochondria with partial loss of cristae, indicative of mitochondrial dysfunction. GPT treatment significantly prevented these ultrastructural disruptions in the cardiac mitochondria of aged

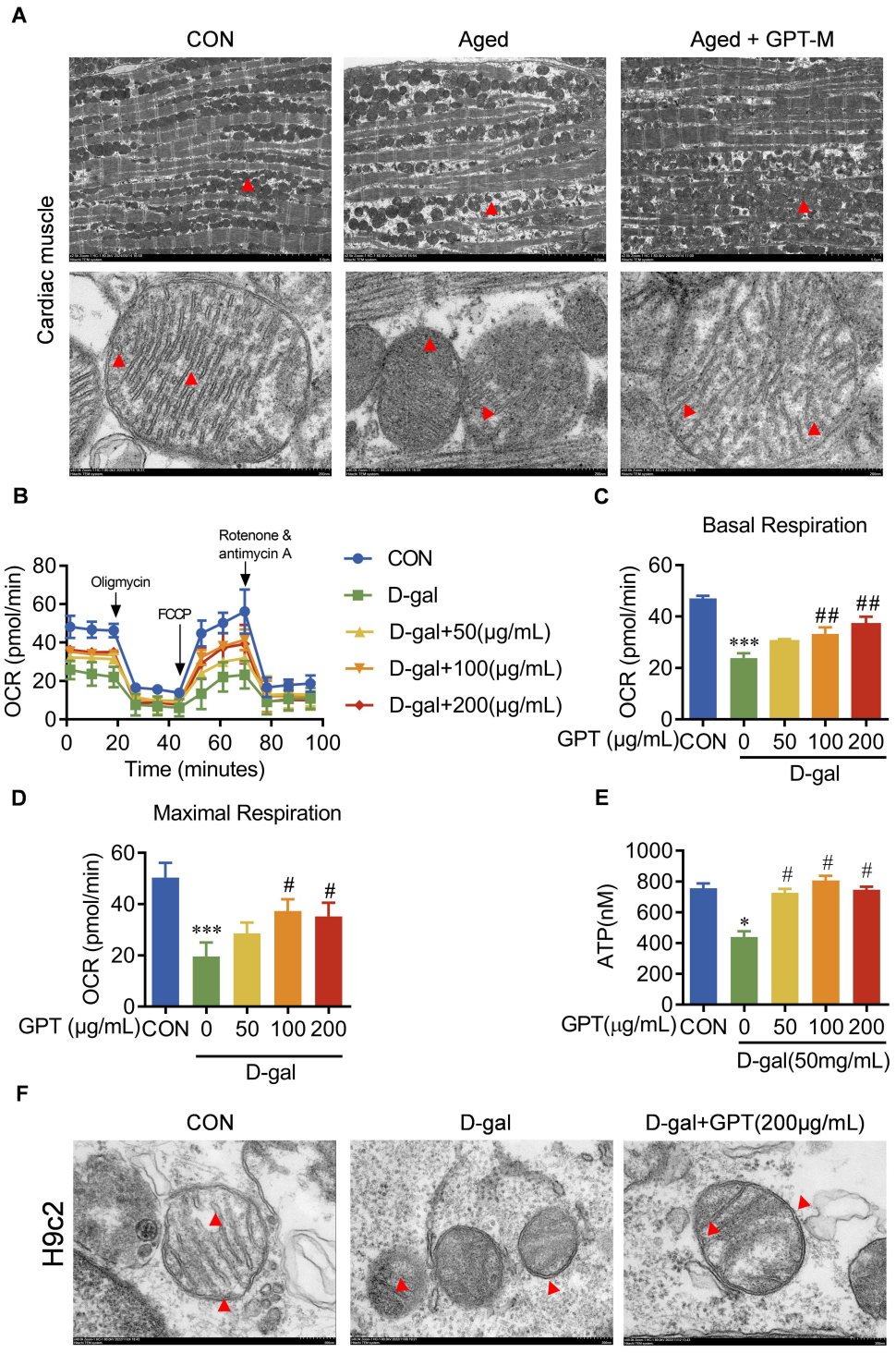

Figure 5 Effect of GPT on mitochondrial function in cardiac muscle of aged mice and D-gal injured H9c2 cells. (**A**) Ultrastructure (2,500×) and electron microscopy images (40,000×) of mitochondria in cardiac muscle. Mitochondrial area statistics (n = 5). (**B**) Seahorse curves of mitochondrial stress experiments in H9c2 cells. (**C** and **D**) Basal respiration and Maximal respiration of Seahorse curves. (**E**) ATP production in H9c2 cells. (**F**) Mitochondrial images (40,000×) and mitochondrial area statistics (n = 3) of H9c2 cells. Compared with control group, $^{*}P < 0.05$, $^{***}P < 0.001$; compared with the model group: $^{\#}P < 0.05$, $^{\#\#}P < 0.01$.

mice (Figure 5A). Seahorse assay results further indicated that D-gal treatment impaired both basal and maximal respiration in cardiac mitochondria, reflecting functional decline. GPT treatment effectively reversed these impairments, restoring mitochondrial respiration to near-normal levels (Figure 5B–D). Similarly, ATP assays showed that GPT treatment increased ATP production in D-gal-injured H9c2 cells (Figure 5E). Electron microscopy of D-gal-injured

https://doi.org/10.2147/DDDT.S509046

H9c2 cells confirmed that GPT treatment mitigated mitochondrial damage, restoring structural integrity (Figure 5F). These findings suggest that GPT exhibits potent efficacy in protecting and improving mitochondrial function in both the cardiac muscle of aged mice and D-gal-injured H9c2 cells, underscoring its potential as a therapeutic agent for age-related mitochondrial dysfunction.

Influence of GPT on Mitochondrial Remodeling in Skeletal Muscle of Aged Mice

Mitochondria undergo continuous fusion and fission to maintain dynamic equilibrium, but this balance is often disrupted during aging.[32] Several key proteins are involved in regulating mitochondrial dynamics, including markers of mitochondrial biosynthesis, such as PGC-1α,[33] PPARγ,[34] Nrf1, as well as fusion marker OPA1,[35] and fission marker Drp1.[36] WB was used to evaluate the levels of these proteins in skeletal muscle (Figure 6A). In aged mice, the expression of these proteins was significantly decreased. Treatment with GPT at low and medium doses (7.5 and 15 g/kg) effectively restored the expression of these proteins, indicating improved mitochondrial biosynthesis and fusion-fission balance. However, the high dose of GPT (30 g/kg) did not provide significant protection against mitochondrial damage in aged mouse skeletal muscles (Figure 6B–F). These results suggest that low and medium doses of GPT have a regulatory effect on mitochondrial remodeling in skeletal muscle, promoting biosynthesis and balancing fusion and fission processes.

Effect of GPT on Cardiac Muscle Mitochondrial Remodeling in Aged Mice

The expression of mitochondrial remodeling markers PGC-1α, PPARγ, Nrf1, OPA1, and Drp1 was also examined in cardiac muscle (Figure 7A). In aged mice, a significant reduction in PGC-1α, PPARγ, Nrf1, and OPA1 was observed, alongside an increase in Drp1, indicating impaired mitochondrial dynamics. Treatment with low and medium doses of GPT (7.5 and 15 g/kg) significantly reversed these changes, promoting mitochondrial biosynthesis and fusion while reducing fission (Figure 7B–F). However, the high dose of GPT (30 g/kg) did not significantly affect the expression of PGC-1α and OPA1. These findings suggest that low and medium concentrations of GPT are effective in promoting mitochondrial biosynthesis and fusion while inhibiting mitochondrial division in the cardiac muscle of aged mice, supporting its role in mitigating age-related mitochondrial dysfunction.

Discussion

As a classic Chinese medicine formula, GPT is often used clinically to treat heart failure,[37] myocardial ischemia,[38] myasthenia gravis,[39] and insomnia. It has also been reported that it can prolong the lifespan of fruit flies,[10] and that the formula contains Huangqi[40] and ginseng[41] which have anti-aging effects in humans. Cycloastragenol is the primary active ingredient of Huangqi and has been shown to have a variety of pharmacological effects, including anti-aging effects, and can also alleviate cardiomyocyte hypertrophy.[42] Rh4, a rare ginsenoside monomer found in ginseng, has potential as a therapeutic agent for delaying skeletal muscle aging by regulating mitochondrial homeostasis.[43] Licorice can delay aging in rats.[44] The polysaccharides in longan[45] and saponins in Yuanzhi[46] can prolong the lifespan of nematodes, while Poria cocos extracts can delay the aging of skin.[47] These studies suggest that GPT has significant potential in slowing the aging process. Based on the traditional effects of GPT in tonifying the spleen and nourishing the heart, we hypothesize that GPT can delay the aging of both skeletal and cardiac muscles. The mouse experiments showed that GPT could mitigate skeletal muscle atrophy in aging mice, together with alleviating cardiac hypertrophy.

Aging is a complex process. It involves a deterioration of physiological pathological functions over time, leading to disease and even death.[48] Although both skeletal and cardiac muscles are muscle tissues, there are many differences between them. Skeletal muscle is under voluntary control,[49] whereas cardiac muscle contracts involuntarily.[50] As the body ages, these muscles undergo distinct changes, in which skeletal muscle tends to atrophy due to increased protein degradation, leading to reduced muscle fiber diameters, while cardiomyocytes proliferate, causing compensatory heart enlargement. GPT counteracts skeletal muscle aging by increasing both the muscle weight and fiber area in aging mice. At the same time, it reduces the heart weight and cardiac fiber area, thereby mitigating cardiac hypertrophy.

Mitochondria are known as energy factories that provide the body with the necessary energy, and mitochondrial dysfunction is considered an important hallmark of aging.[51] Skeletal and cardiac muscle include some of the most important tissues in the human body[52] and are associated with high mitochondrial contents.[53] The imbalance in

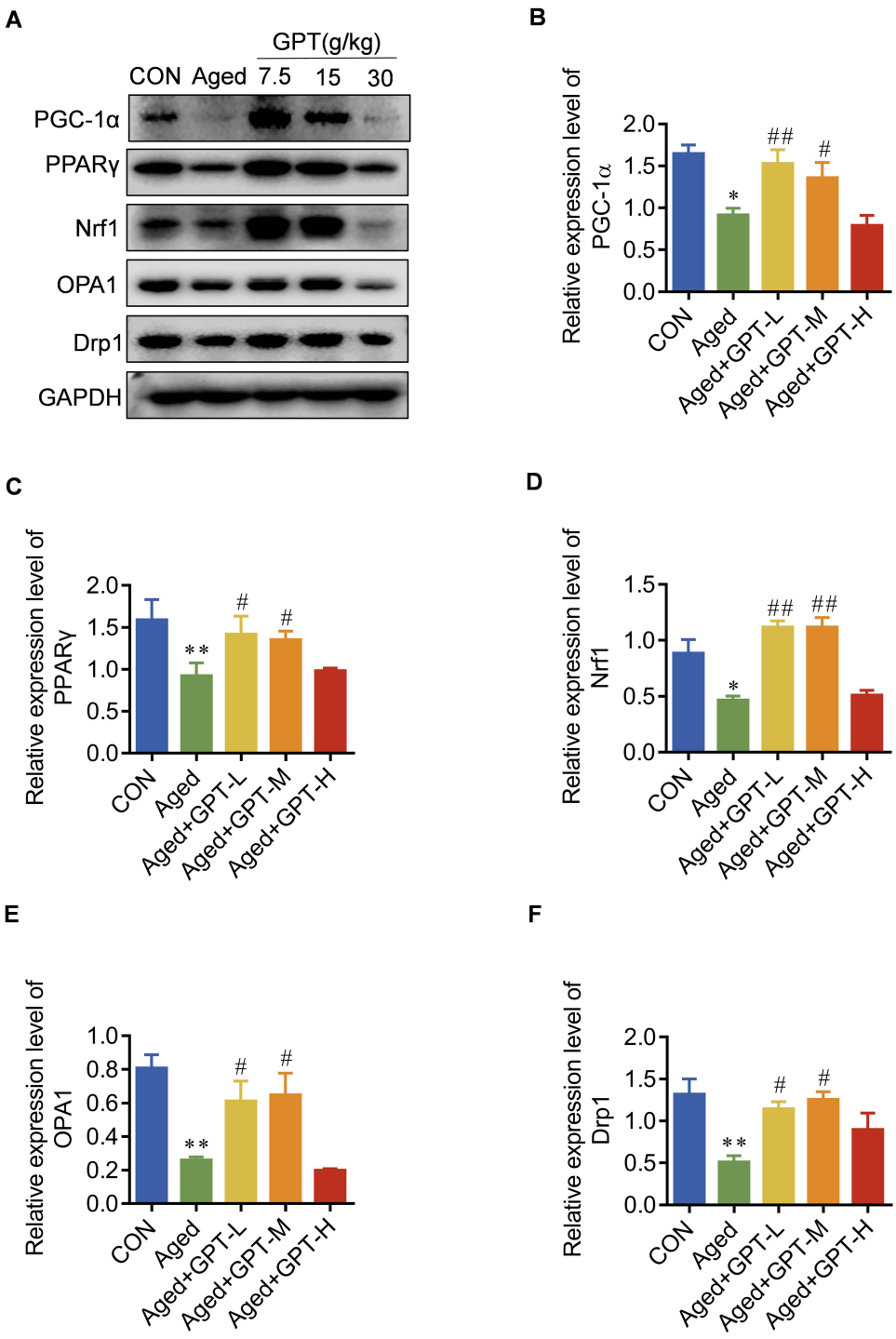

Figure 6 The influence of GPT on mitochondrial remodeling in skeletal muscles of aged mice. (**A**) Protein levels of PGC-1α, PPARγ, OPA1, Drp1, and Nrf1 were evaluated by Western blot. (**B**–**F**) Densitometry was used to quantify PGC-1α, PPARγ, OPA1, Drp1, and Nrf1 levels. Data (n=3) represent means ± SD. Compared with control group: $^{*}P < 0.05$, $^{**}P < 0.01$; compared with model group: $^{\#}P < 0.05$, $^{\#\#}P < 0.01$.

mitochondrial homeostasis that accompanies the aging process can lead to loss of skeletal muscle mass[54] and impaired cardiac function.[55] Abnormal increases in the number of mitochondria, accompanied by rupture of the mitochondrial membranes, lysis of the internal cristae, and even vacuolization have been observed in aging mice.[30] The dynamic homeostasis of the mitochondria is closely associated with their biosynthesis, fusion, division and autophagy. PPARγ is one of the three types of peroxisome proliferator activators (PPARs), and constitutive overexpression of PPARγ in mouse

https://doi.org/10.2147/DDDT.S509046

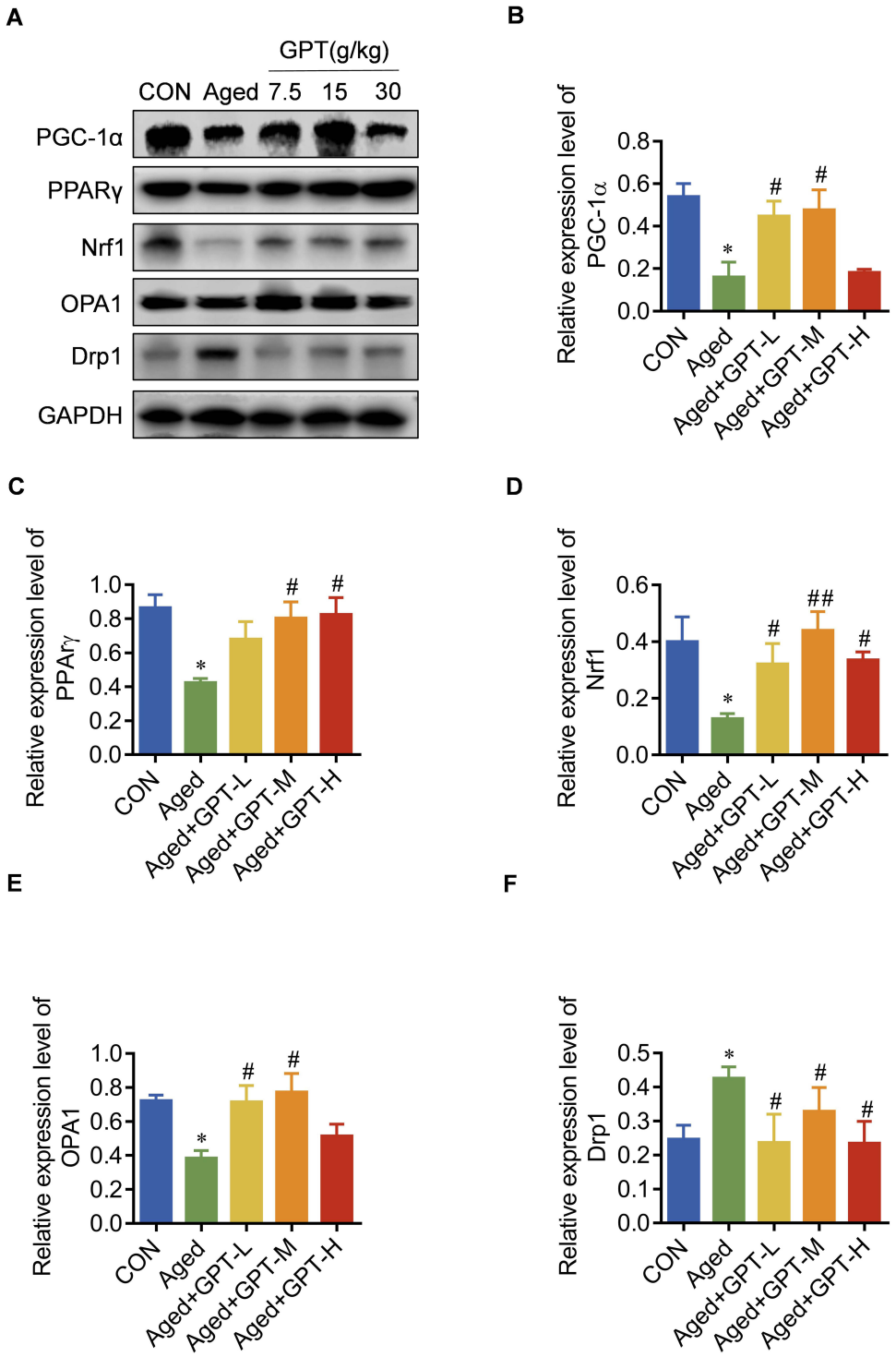

Figure 7 The effects of GPT on mitochondrial remodeling in cardiac muscle of aged mice. (**A**) Protein expression of PGC-1α, PPARγ, OPA1, Drp1, and Nrf1 were evaluated by Western blot. (**B**–**F**) Densitometry was used to quantify PGC-1α, PPARγ, OPA1, Drp1, and Nrf1 levels. Data (n=3) represent means ± SD. Compared with control group: $^{*}P < 0.05$; compared with model group: $^{\#}P < 0.05$, $^{\#\#}P < 0.01$.

skeletal muscle induces lipocalin production in muscle, reduces muscle atrophy, and increases the content of oxidized muscle fibers, as well as enhancing insulin sensitivity.[7] Nuclear respiratory factor 1 (NRF-1) binds specifically to sites in the promoter regions of several nuclear genes required for mitochondrial respiration-promoted transcription, and activated PGC-1α, together with PPARγ, enhances the transcriptional activity of NRF1 to drive mitochondrial biogenesis

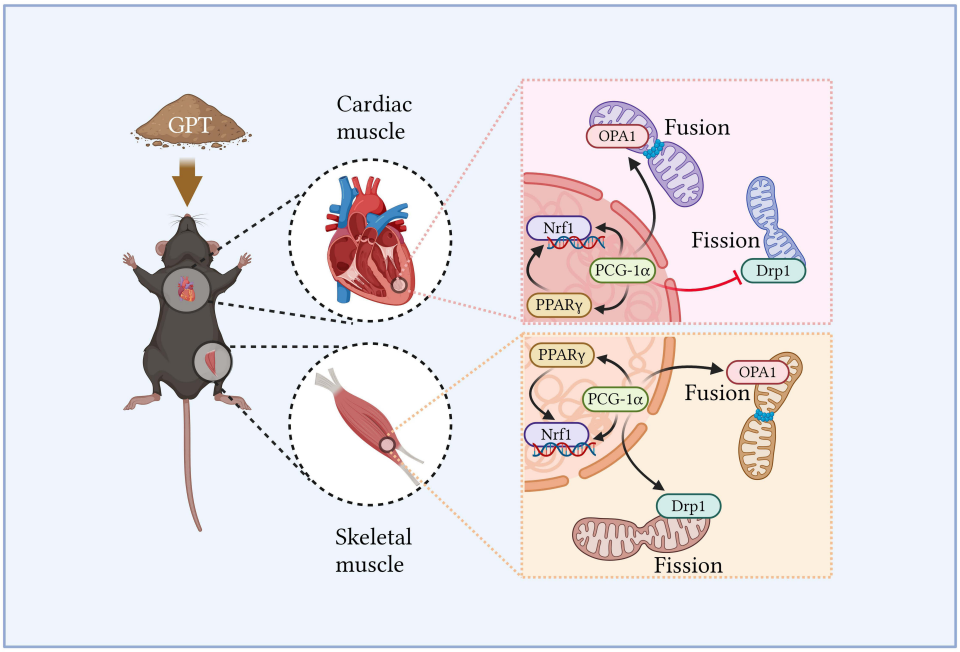

Figure 8 GPT slows skeletal muscle and cardiac muscle aging by promoting mitochondrial remodeling.

and the expression of adaptive metabolic genes.[56] The mitochondrial fusion protein OPA1 has been shown to be regulated by PGC-1α,[7] and PGC-1α also regulates Drp1-mediated mitochondrial fission directly by binding to the Drp-1 transcriptional promoter.[57] Our experiments showed that GPT significantly influences the expression of PGC-1α, PPARγ, Nrf1, OPA1, and Drp1, with stronger effects observed at low and medium doses. The phenomenon may have been due to different optimal concentration ranges of the various compounds, with upper dosing limits beyond which their effects plateau or decline.[58]

It has been shown that both overall aging and the rate of aging are synchronized among different tissues, although the specific mechanisms differ according to tissue type.[56] Atrophy of skeletal muscle fibers occurs during aging of the muscle, accompanied by reduced expression of the mitochondrial fusion protein OPA1 and fission protein Drp1,[52] suggesting an imbalance in the fusion and fission of skeletal muscle mitochondria. However, the situation in cardiac muscle differs, as reduced mitochondrial fusion is complicated by cardiomyocyte hypertrophy and mitochondrial dysfunction leading to heart failure.[7] Reduced mitochondrial fusion and increased expression of Drp1[56] disrupt the overall balance of mitochondrial dynamics, thus demonstrating significant differences in the mechanisms associated with skeletal and cardiac muscle aging (Figure 8).

Conclusion

In summary, the experiments demonstrate that GPT can regulate mitochondrial remodeling and mitigate skeletal and cardiac muscle damage in aged mice. Notably, GPT exerts distinct effects on these tissues: in skeletal muscle, GPT promotes mitochondrial biosynthesis, fusion, and division, thereby increasing mitochondrial remodeling and offering protection to the muscle. In cardiac muscle, GPT promotes mitochondrial biosynthesis and fusion while inhibiting mitochondrial fission, thus maintaining mitochondrial homeostasis and protecting cardiac muscle. This study provides important experimental evidence supporting the potential of GPT in delaying the aging process of both skeletal and cardiac muscle.

Abbreviations

ATP, Adenosine triphosphate; CSA, Cross-sectional area; D-gal, D-galactose; Drp1, Dynamin-related protein 1; FCCP, Carbonyl cyanide 4-(trifluoromethoxy) phenylhydrazone; GPT, Gui-Pi-Tang; GPT-H, GPT high dose group; GPT-L, GPT

https://doi.org/10.2147/DDDT.S509046

low dose group; GPT-M, GPT medium dose group; Nrf1, Nuclear respiratory factor 1; OCR, Oxygen Consumption Rate; OPA1, Optic atrophy 1; PGC-1α, Peroxisome proliferator-activated receptor-γ coactlvator-1α; PPARγ, Peroxisome proliferator-activated receptor γ; SA-β-gal, SPiDER-β-galactosidase.

Data Sharing Statement

The original contributions presented in the study are included in the article/supplementary material, further inquiries can be directed to the corresponding authors.

Animal Ethics Statement

All animal procedures were performed following the principles approved by the Animal Ethics Committee of Changchun University of Chinese Medicine. Our study strictly adhered to the National Research Council's Guide for the Care and Use of Laboratory Animals (8th edition, 2011) and the ARRIVE guidelines (Animal Research: Reporting of In Vivo Experiments). (approval no 2022476).

Acknowledgments

The authors would like to thank all the reviewers who participated in the review and MJEditor (www.mjeditor.com) for its linguistic assistance during the preparation of this manuscript.

Author Contributions

All authors made a significant contribution to the work reported, whether that is in the conception, study design, execution, acquisition of data, analysis and interpretation, or in all these areas; took part in drafting, revising or critically reviewing the article; gave final approval of the version to be published; have agreed on the journal to which the article has been submitted; and agree to be accountable for all aspects of the work.

Funding

This work was supported by the Science and Technology Development of Jilin Province (YDZJ202301ZYTS453) and the National Natural Science Foundation of China (No. 82204709).

Disclosure

The authors report no conflicts of interest in this work.

References

1. de Oliveira Zanuso B, de Oliveira Dos Santos AR, Miola VFB, Guissoni Campos LM, Spilla CSG, Barbalho SM. Panax ginseng and aging related disorders: a systematic review (1873-6815 (Electronic)). *Exper Gerontol*. 2022;161:111731.
2. Guo J, Huang X, Dou L, et al. Aging and aging-related diseases: from molecular mechanisms to interventions and treatments. *Signal Transduct Target Ther*. 2022;7(1):391. doi:10.1038/s41392-022-01251-0
3. López-Otín C, Blasco MA, Partridge L, Serrano M, Kroemer G. Hallmarks of aging: an expanding universe. *Cell*. 2023;186(2):243–278. doi:10.1016/j.cell.2022.11.001
4. Liu SZ, Marcinek DJ. Skeletal muscle bioenergetics in aging and heart failure. *Heart Fail Rev*. 2017;22(2):167–178. doi:10.1007/s10741-016-9586-z
5. Rosen RS, Yarmush ML. Current trends in anti-aging strategies. *Annu Rev Biomed Eng*. 2023;25(1):363–385. doi:10.1146/annurev-bioeng-120122-123054
6. Liu YJ, McIntyre RL, Janssens GE, Houtkooper RH. Mitochondrial fission and fusion: a dynamic role in aging and potential target for age-related disease. *Mech Ageing Dev*. 2020;186:111212. doi:10.1016/j.mad.2020.111212
7. Bernhardt D, Müller M, Reichert AS, Osiewacz HD. Simultaneous impairment of mitochondrial fission and fusion reduces mitophagy and shortens replicative lifespan. *Sci Rep*. 2015;5(1):7885. doi:10.1038/srep07885
8. Chaudhari SN, Kipreos ET. Increased mitochondrial fusion allows the survival of older animals in diverse C. elegans longevity pathways. *Nat Commun*. 2017;8(1):182. doi:10.1038/s41467-017-00274-4
9. Tepp K, Timohhina N, Puurand M, et al. Bioenergetics of the aging heart and skeletal muscles: modern concepts and controversies. *Ageing Res Rev*. 2016;28:1–14. doi:10.1016/j.arr.2016.04.001
10. Liang Y, Wang Y, Wang KM. Regulation of Drosophila life-span and anti-oxidantion by guipi decoction. *Guangdong Chem Indu*. 2017;44(20):215–218.

11. Lei P, Song YX, Xu XZ, et al. Effects of guipi decoction on oxidative stress and mitophagy related proteins CIF model induced by 5-FU. *Lishizhen Med Materia Medica Res*. 2024;35(03):593–597.
12. Zhou WJ, Chai Z, Wang YH, et al. Influence of CYP3A4 activity of guipi tang to acute liver injury induced by extract from tripterygium wilfordii by ethanol. *Chin J Exper Trad Med Formulae*. 2015;21(06):113–116. doi:10.13422/j.cnki.syfjx.2015060113
13. Wang M, Chen X, Yan X, et al. Jie-Du-Tong-Luo formula protects C2C12 myotubes against high glucose and palmitic acid injury by activating the PI3K/Akt/PPARgamma pathway in vitro. *Heliyon*. 2024;10(15):e35423. doi:10.1016/j.heliyon.2024.e35423
14. Zhang J, Luo L, Guo Y, et al. Pharmacological effects and target analysis of guipi wan in the treatment of cerebral ischemia-reperfusion injury. *Front Pharmacol*. 2024;15:1346226. doi:10.3389/fphar.2024.1346226
15. Xiang G, Ying K, Jiang P, et al. Growth differentiation factor 11 induces skeletal muscle atrophy via a STAT3-dependent mechanism in pulmonary arterial hypertension. *Skelet Muscle*. 2022;12(1):10. doi:10.1186/s13395-022-00292-x
16. Wang M, Jiang R, Liu J, et al. 20(s)ginsenosideRg3 modulation of AMPK/FoxO3 signaling to attenuate mitochondrial dysfunction in a dexamethasoneinjured C2C12 myotube-based model of skeletal atrophy in vitro. *Mol Med Rep*. 2021;23(5). doi:10.3892/mmr.2021.11945
17. Huang Q, Su H, Qi B, et al. A SIRT1 Activator, Ginsenoside Rc, Promotes Energy Metabolism in Cardiomyocytes and Neurons. *J Am Chem Soc*. 2021;143(3):1416–1427. doi:10.1021/jacs.0c10836
18. Liu J, Peng Y, Wang X, et al. Mitochondrial dysfunction launches dexamethasone-induced skeletal muscle atrophy via AMPK/FOXO3 signaling. *Mol Pharm*. 2016;13(1):73–84. doi:10.1021/acs.molpharmaceut.5b00516
19. Qi W, Xu X, Wang M, et al. Inhibition of Wee1 sensitizes AML cells to ATR inhibitor VE-822-induced DNA damage and apoptosis. *Biochem Pharmacol*. 2019;164:273–282. doi:10.1016/j.bcp.2019.04.022
20. Wei WL, Zeng R, Gu CM, Qu Y, Huang LF. Angelica sinensis in China-A review of botanical profile, ethnopharmacology, phytochemistry and chemical analysis. *J Ethnopharmacol*. 2016;190:116–141. doi:10.1016/j.jep.2016.05.023
21. Ru W, Wang D, Xu Y, et al. Chemical constituents and bioactivities of Panax ginseng (C.A. Mey). *Drug Discov Ther*. 2015;9(1):23–32. doi:10.5582/ddt.2015.01004
22. Zhu B, Zhang QL, Hua JW, Cheng WL, Qin LP. The traditional uses, phytochemistry, and pharmacology of Atractylodes macrocephala Koidz.: a review. *J Ethnopharmacol*. 2018;226:143–167. doi:10.1016/j.jep.2018.08.023
23. Tang YY, He XM, Sun J, et al. Polyphenols and alkaloids in byproducts of longan fruits (Dimocarpus Longan Lour.) and their bioactivities. *Molecules*. 2019;24(6):10.3390/molecules24061186.
24. Huang G, Tong Y, He Q, Wang J, Chen Z, Aucklandia Lappa DC. extract enhances gefitinib efficacy in gefitinib-resistance secondary epidermal growth factor receptor mutations. *J Ethnopharmacol*. 2017;206:353–362. doi:10.1016/j.jep.2017.06.011
25. Xiao Y, Han F, Lee IS. Biotransformation of the phenolic constituents from licorice and cytotoxicity evaluation of their metabolites. *Int J mol Sci*. 2021;22(18):10.3390/ijms221810109.
26. Gong L, Xie JB, Luo Y, et al. Research progress of quality control for the seed of Ziziphus jujuba var. spinosa (Bunge) Hu ex H.F. Chow (Suan-Zao-Ren) and its proprietary Chinese medicines. *J Ethnopharmacol*. 2023;307:116204. doi:10.1016/j.jep.2023.116204
27. Zhao X, Cui Y, Wu P, et al. Polygalae Radix: a review of its traditional uses, phytochemistry, pharmacology, toxicology, and pharmacokinetics. *Fitoterapia*. 2020;147:104759. doi:10.1016/j.fitote.2020.104759
28. Wang P, Wang Z, Zhang Z, et al. A review of the botany, phytochemistry, traditional uses, pharmacology, toxicology, and quality control of the *Astragalus memeranaceus*. *Front Pharmacol*. 2023;14:1242318. doi:10.3389/fphar.2023.1242318
29. Doura T, Kamiya M, Obata F, et al. Detection of Lacz-positive cells in living tissue with single-cell resolution. *Angew Chem Int Ed Engl*. 2016;55 (33):9620–9624. doi:10.1002/anie.201603328
30. Huang DD, Fan SD, Chen XY, et al. Nrf2 deficiency exacerbates frailty and sarcopenia by impairing skeletal muscle mitochondrial biogenesis and dynamics in an age-dependent manner. *Exp Gerontol*. 2019;119:61–73. doi:10.1016/j.exger.2019.01.022
31. Wang HH, Sun YN, Qu TQ, et al. Nobiletin prevents D-galactose-induced C2C12 cell aging by improving mitochondrial function. *Int J mol Sci*. 2022;23(19). doi:10.3390/ijms231911963
32. Wang S, Tan J, Miao Y, Zhang Q. Mitochondrial dynamics, mitophagy, and mitochondria-endoplasmic reticulum contact sites crosstalk under hypoxia. *Front Cell Dev Biol*. 2022;10:848214. doi:10.3389/fcell.2022.848214
33. Han JW, Shin SK, Bae HR, et al. Wheat seedlings extract ameliorates sarcopenia in aged mice by regulating protein synthesis and degradation with anti-inflammatory and mitochondrial biogenesis effects. *Phytomedicine*. 2024;130:155747. doi:10.1016/j.phymed.2024.155747
34. Manickam R, Duszka K, Wahli W. PPARs and microbiota in skeletal muscle health and wasting. *Int J mol Sci*. 2020;21(21):8056. doi:10.3390/ijms21218056
35. Noone J, Dj O, Kenny HC. OPA1 regulation of mitochondrial dynamics in skeletal and cardiac muscle. *Trends Endocrinol Metab*. 2022;33 (10):710–721. doi:10.1016/j.tem.2022.07.003
36. Leduc-Gaudet JP, Hussain SNA, Barreiro E, Gouspillou G. Mitochondrial dynamics and mitophagy in skeletal muscle health and aging. *Int J mol Sci*. 2021;22(15):8179. doi:10.3390/ijms22158179
37. Liang YC, Chen SC, Li XW, et al. GuiPi decoction regulates autophagy of H9c2 cardiomyocytes exposed to high glucose via Bmal1. *Pharmacol Clin Chin Materia Medica*. 2022;38(06):42–47. doi:10.13412/j.cnki.zyyl.2022.06.009
38. Wu JL, Jia YT, Dai C, et al. Effect of Guipitang on ERK1/2 and p38 MAPK on rats with myocardial ischemia. *Chin J Exper Trad Med Formulae*. 2024;30(02):1–8. doi:10.13422/j.cnki.syfjx.20230905
39. Song YX, Lei P, Wei DS, Wang Y, Ma XD. Experimental study on the anti-inflammatory mechanism of guipi decoction on myasthenia rats after chemotherapy. *J Hainan Med Univ*. 2024;30(12):921–929. doi:10.13210/j.cnki.jhmu.20240329.002
40. Li H, Xu J, Zhang Y, et al. Astragaloside IV alleviates senescence of vascular smooth muscle cells through activating parkin-mediated mitophagy. *Hum Cell*. 2022;35(6):1684–1696. doi:10.1007/s13577-022-00758-6
41. Tian T, Ko CN, Luo W, Li D, Yang C. The anti-aging mechanism of ginsenosides with medicine and food homology. *Food Funct*. 2023;14 (20):9123–9136. doi:10.1039/d3fo02580b
42. Wang J, Wu ML, Cao SP, Cai H, Zhao ZM, Song YH. Cycloastragenol ameliorates experimental heart damage in rats by promoting myocardial autophagy via inhibition of AKT1-RPS6KB1 signaling. *Biomed Pharmacother*. 2018;107:1074–1081. doi:10.1016/j.biopha.2018.08.016
43. Zhu A, Duan Z, Chen Y, Zhu C, Fan D. Ginsenoside Rh4 delays skeletal muscle aging through SIRT1 pathway. *Phytomedicine*. 2023;118:154906. doi:10.1016/j.phymed.2023.154906

44. Zhao F, Gao L, Qin X, Du G, Zhou Y. The intervention effect of licorice in d-galactose induced aging rats by regulating the taurine metabolic pathway. *Food Funct*. 2018;9(9):4814–4821. doi:10.1039/c8fo00740c
45. Guo X, Xin Q, Wei P, et al. Antioxidant and anti-aging activities of Longan crude and purified polysaccharide (LP-A) in nematode Caenorhabditis *elegans*. *Int J Biol Macromol*. 2024;267(Pt 2):131634. doi:10.1016/j.ijbiomac.2024.131634
46. Zeng W, Wu AG, Zhou XG, et al. Saponins isolated from radix polygalae extent lifespan by modulating complement C3 and gut microbiota. *Pharmacol Res*. 2021;170:105697. doi:10.1016/j.phrs.2021.105697
47. Fang CL, Paul CR, Day CH, et al. Poria cocos (Fuling) targets TGFβ/Smad7 associated collagen accumulation and enhances Nrf2-antioxidant mechanism to exert anti-skin aging effects in human dermal fibroblasts. *Environ Toxicol*. 2021;36(5):729–736. doi:10.1002/tox.23075
48. Larsson L, Degens H, Li M, et al. Sarcopenia: aging-related loss of muscle mass and function. *Physiol Rev*. 2019;99(1):427–511. doi:10.1152/physrev.00061.2017
49. Coen PM, Huo Z, Tranah GJ, et al. Autophagy gene expression in skeletal muscle of older individuals is associated with physical performance, muscle volume and mitochondrial function in the study of muscle, mobility and aging (SOMMA). *Aging Cell*. 2024;23(6):e14118. doi:10.1111/acel.14118
50. Qian L, Xu H, Yuan R, Yun W, Ma Y. Formononetin ameliorates isoproterenol induced cardiac fibrosis through improving mitochondrial dysfunction. *Biomed Pharmacother*. 2024;170:116000. doi:10.1016/j.biopha.2023.116000
51. Suomalainen A, Nunnari J. Mitochondria at the crossroads of health and disease. *Cell*. 2024;187(11):2601–2627. doi:10.1016/j.cell.2024.04.037
52. Boengler K, Kosiol M, Mayr M, Schulz R, Rohrbach S. Mitochondria and ageing: role in heart, skeletal muscle and adipose tissue. *J Cachexia Sarcopenia Muscle*. 2017;8(3):349–369. doi:10.1002/jcsm.12178
53. Goyal P, Maurer MS, Roh J. Aging in heart failure: embracing biology over chronology: JACC family series. *JACC Heart Fail*. 2024;12(5):795–809. doi:10.1016/j.jchf.2024.02.021
54. De Mario A, Gherardi G, Rizzuto R, Mammucari C. Skeletal muscle mitochondria in health and disease. *Cell Calcium*. 2021;94:102357. doi:10.1016/j.ceca.2021.102357
55. Xie S, Xu SC, Deng W, Tang Q. Metabolic landscape in cardiac aging: insights into molecular biology and therapeutic implications. *Signal Transduct Target Ther*. 2023;8(1):114. doi:10.1038/s41392-023-01378-8
56. Alibhai FJ, Li RK. Rejuvenation of the aging heart: molecular determinants and applications. *Can J Cardiol*. 2024;40(8):1394–1411. doi:10.1016/j.cjca.2024.03.004
57. Cheng YH, Lin FH, Wang CY, et al. Recovery of oxidative stress-induced damage in Cisd2-deficient cardiomyocytes by sustained release of ferulic acid from injectable hydrogel. *Biomaterials*. 2016;103:207–218. doi:10.1016/j.biomaterials.2016.06.060
58. Huang Y, Zhang Y, Wu Y, Xiang Q, Yu R. An integrative pharmacology-based strategy to uncover the mechanism of Zuogui Jiangtang Shuxin formula in diabetic cardiomyopathy. *Drug Des Devel Ther*. 2023;17:237–260. doi:10.2147/dddt.S390883